ICFM 10
Adapting to Global Change:
Innovative Approaches to Flood Management and Resilience
May 20-22, 2026 | Western University, London, Ontario, Canada

Approach for Assessing Land-Cover Changes using Satellite Imagery and their Impact on Risk of Flooding

Badri Bhakta Shrestha[1,*], Mohamed Rasmy[1], Katsunori Tamakawa[2], Sauhardra Joshi[3] and Daisuke Kuribayashi[1]

International Centre for Water Hazard and Risk Management (ICHARM), Public Works Research Institute (PWRI), Tsukuba, 305-8516, Japan[1]

[*]Correspondence E-mail: shrestha@icharm.org

Global Environment Data Commons, The University of Tokyo, Tokyo, 153-8505, Japan[2]

Department of Hydrology and Meteorology, Ministry of Energy, Water Resources and Irrigation, Kathmandu, 44600, Nepal[3]

ABSTRACT

It is crucial to understand land-cover changes and their impacts on society because land-use and land-cover (LULC) changes have recently become a key component in flood risk management. Most previous studies mainly analyzed the impact of land-cover changes on surface runoff or river discharge, and limited research investigated their impact on flood risk, including flood extent and volume. This study thus aimed to analyze land-cover changes and their impact on flood risk and hydrological responses, including flood runoff, inundation, and volume, in the Bagmati River basin of Nepal. Land-cover maps for historical years (2014, 2019, and 2024) were generated using Landsat satellite imagery in the Google Earth Engine Platform, and land-cover maps for future years were projected using machine learning techniques. After preparing land-cover maps, flood simulations were conducted for flood events of different return periods using a diffusive-wave based distributed hydrologic-hydraulic model named the Rainfall Runoff Inundation (RRI) model with the land-cover maps for different years. Then, we analyzed the impact of LULC changes on flood runoff, flood inundation, flood inundation volume, and flood risk. The results show that the built-up area may increase by 73% in the future, while the cropland area may decrease by 28%. The flood inundation extent and the peak inundation volume for a 100-year flood may increase by 2.5% and 4.7% in the future. The inundated built-up area may increase by more than 79% under LULC conditions in 2049, while the flood-exposed area of cropland may decrease by 6.3%. The results of this study can be useful for planning and implementing effective flood risk reduction measures and for establishing land use planning and regulations.

KEYWORDS: land use/land cover, flood inundation, exposure, RRI model, Nepal flood

1 INTRODUCTION

Floods are one of the most common water-related disasters in the world. Flood risk has been increasing in many countries (Zhai et al., 2005), particularly developing ones, due to rapidly growing settlement areas, poorly planned development activities, continuous land-use and land-cover (LULC) changes, and ongoing climate change. Among these, LULC changes have recently been recognized as a major environmental issue, affecting hydrological characteristics and society. They are regarded as significantly altering the natural water cycle and the spatial distribution of surface runoff, thereby impacting flow discharge and, consequently, increasing flood risk. In addition, changes in the land system in flood-prone areas may expose them to even greater environmental risks. It is thus crucial to understand

land-cover changes and their impacts on hydrological responses and society to better manage flood risk in the future and establish effective land-use regulations.

Accurately understanding flood characteristics and flood risk levels while considering potential LULC changes provides useful information to effectively carry out future flood management and establish land use regulations. Moreover, urbanization and LULC changes may have significant impacts on hydrological responses in the watershed (e.g., river runoff and flood inundation) and on flood risk (Martínez-Retureta et al., 2020). LULC changes can be analyzed using satellite imagery (Shrestha, 2019a), and their impact on hydrological responses can be assessed by incorporating land-cover maps for different years into hydrological model simulations. Numerous studies have focused on the analysis of LULC impact on hydrological responses (Shrestha, 2019a; Martínez-Retureta et al., 2020; Wudineh, 2023; Banjara et al., 2024). However, most of them have mainly analyzed its impact on river runoff, and limited research has investigated its impact on flood inundation (Shrestha, 2019a). Understanding the impact of LULC changes while considering potential future land-use changes is crucial to implementing better land-use management practices and providing policy- and decision-makers with useful information to identify flood risk levels and plan and enforce appropriate land-use regulations.

This study presents a novel integration of machine learning–based future land-cover projections with hydrological flood modeling to assess the impacts of LULC changes on flood dynamics and risk. We analyzed LULC changes and their impacts on flood risk and hydrological responses, including flood runoff, inundation, and volume, in the Bagmati River basin of Nepal. The land-cover maps for 2014, 2019, and 2024 were generated from Landsat satellite imagery using the Google Earth Engine (GEE) Platform. The land-cover changes were analyzed using a Geographic Information System (GIS), and future land-cover maps were projected using machine learning techniques with a QGIS plugin called the Modules of Land Use Change Evaluation (MOLUSCE). After preparing land-cover maps, flood simulations were conducted for flood events of different return periods using the Rainfall-Runoff-Inundation (RRI) model with the land-cover maps generated for the past years and projected maps for the future years. Then, we investigated the impact of LULC changes on flood runoff, inundation, and volume. By overlaying the land-cover maps with delineated flood inundation maps in GIS, we also estimated the flood-exposed area for each land-cover class to assess their flood risk.

2 STUDY AREA

Figure 1 shows the location of the Bagmati River basin of Nepal and its topographical features. The watershed area within the study boundary is approximately 4723 km^2, including the Lal Bakaiya River basin. The figure also shows the location of the water level stations. The elevation of the basin ranges from 72.4 to 2843 m. The average annual precipitation in the basin is approximately 1805 mm, and more than 81% rainfall occurs in the monsoon season (June-September). The Bagmati River basin is important in Nepal for its cultural, religious and economic significance. However, this basin has recently been experiencing severe flooding, resulting in significant physical damage and agricultural crop losses. Therefore, it is crucial to understand LULC changes and their impacts on flooding and flood risk in the basin to manage future flood risk better.

3 DATA AND METHODOLOGY

The key terminologies in this study are defined as follows: (i) *hydrology* refers to the study of the occurrence, distribution, and movement of water within the Earth system, including processes such as precipitation, runoff, infiltration, and river discharge; (ii) *hazard* refers to the potential occurrence of flood inundation under different scenarios; (iii) *inundation* refers to the resulting flooding of normally dry land and is characterized by the spatial extent and depth of floodwater; and (iv) *risk* is defined as a function of hazard probability and exposure, where exposure is influenced by LULC dynamics. This study consisted of two components: (i) analysis of land-cover changes and projection of future land-cover

maps, and (ii) assessment of the impact of LULC changes on flood risk and hydrological responses, including flood runoff, inundation, and volume (Figure 2). The methodology and data used for this study are described in the following subsections.

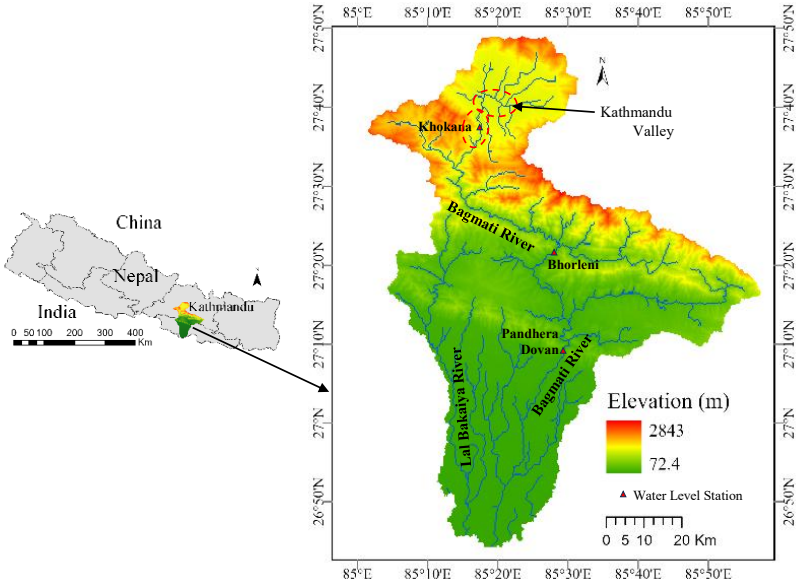

Figure 1: Location of the Bagmati River basin, Nepal

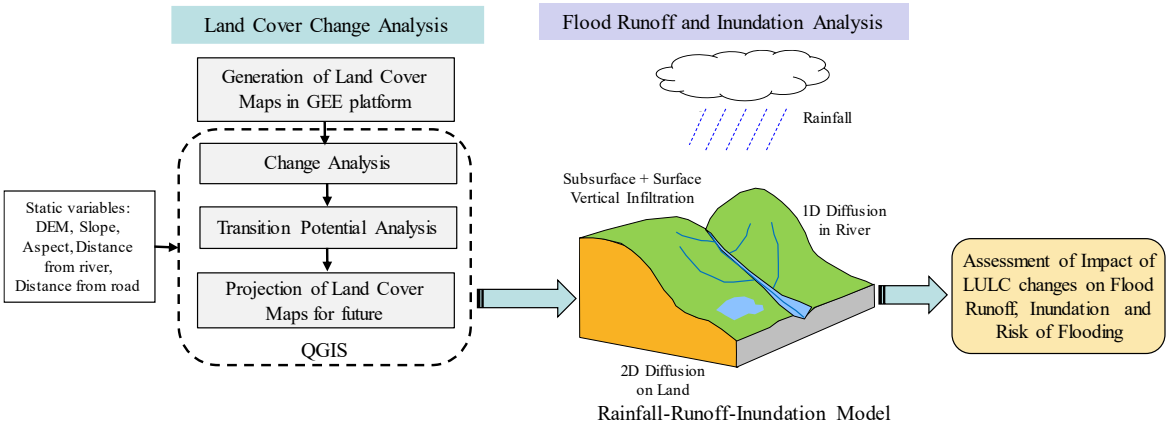

Figure 2: Methodology used in this study

3.1 Analysis of Land-Use and Land-Cover Changes

We generated land-cover maps for 2014, 2019, and 2024 using Landsat 8 surface reflectance images (USGS Landsat 8 Level 2, Collection 2, Tier 1) of 1 arc-second spatial resolution with the GEE Platform (Earth Resources Observation and Science Center, 2020). Images with less than 4% cloud cover were collected. To generate training and validation samples, true-color (RGB bands 432) and false-color (RGB bands 543) composite images were created using the multiband Landsat images. This study used a supervised classification method, which requires the development of training sites. The land-cover categories in the basin were classified into six classes: 1) Water bodies, 2) Forest, 3) Vegetation, 4) Bare land, 5) Cropland, and 6) Built-up areas. Training and validation samples for each land-cover class in 2014, 2019, and 2024 were created throughout the entire image based on composite and Google Earth images. Total number of selected training samples for land cover class for 2014, 2019, and 2024 was about 800, 812, and 885, respectively, while the total selected validation samples were 180 for 2014, 184 for 2019, and 215 for 2024. The random forest classifier available in the GEE platform was used to

generate a land-cover map from the training samples. Accuracy assessment was conducted using the validation samples for each generated map. A land-cover map for 2004 was also generated for calibrating hydrologic-hydraulic model simulations. The spatial resolution of the generated land-cover maps for the past years was upscaled from 1 arc-second to 9 arc-seconds, which is the same resolution as the hydrologic-hydraulic model simulations.

To analyze LULC changes and project future land-cover maps, we used a QGIS plugin called the MOLUSCE. The land cover maps for 2014 and 2019 were used to train the MOLUSCE model, and the land cover map for 2024 was used to validate the model. The cellular automata-artificial neural network model in the MOLUSCE was used for projecting future land-cover maps. The transition matrix and change map of the land-cover maps between 2014 and 2019, as well as static variables, such as digital elevation model (DEM), slope, aspect, distance from the river, and distance from the major road, were used to train the model. The DEM data were downloaded from the HydroSHEDS (Lehner et al., 2008). The slope and aspect were calculated using DEM in GIS. The river network data were delineated by referring to Google Earth images in GIS. The road data were downloaded from the Humanitarian Data Exchange of UN-OCHA, which was developed by the Overture Maps Organization (Overture Maps Foundation, 2025). First, a land-cover map for 2024 was projected and validated with the generated land-cover map using the validation module in the MOLUSCE. The LULC projected model performance was in an acceptable range with 77% overall accuracy and 0.65 kappa values. Then, land-cover maps for future years, 2039 and 2049, were projected.

3.2 Analysis of the Impact of Land-Use and Land-Cover Changes on Flood Risk

Flood simulations were conducted using the RRI model, a diffusive-wave based distributed hydrologic-hydraulic model, with the land-cover maps generated for past years and projected maps for the future years. To simulate past flood events, observed rainfall from ground-gauge stations across the basin was used as input to the model. The values of the model parameters were defined considering land-cover classes to analyze the impact of LULC changes on flooding and hydrological responses in the study basin. The RRI model is a two-dimensional hydrologic-hydraulic model capable of simulating rainfall-runoff, infiltration process, and flood inundation simultaneously (Sayama et al., 2012). The model was set up for the basin with DEM data of 9 arc-seconds (approximately 270 m spatial resolution). The HydroSHEDS DEM of 3 arc-seconds was upscaled to 9 arc-seconds for smooth simulations of the RRI model. The model was calibrated and validated using past flood data by comparing calculated and observed discharges (calibration used 2004 flood data; validation used 2002, 2014, and 2019 flood data). The model was also validated by comparing calculated flood extent areas with satellite based flood observation. Then, flood simulations were conducted for a recent severe flood event in 2024 (11-year flood) and flood events of different return periods (50- and 100-year floods), using the land-cover map created for 2024 and the land-cover maps projected for 2039 and 2049. For designing the spatial and temporal rainfall for different return periods, flood frequency analysis was performed using basin average 2-day annual maximum rainfall data from 1976 to 2024, based on the Generalized Extreme Value (GEV) distribution. Rainfall for specific return periods (e.g., 50- and 100-year floods) was generated using the spatial and temporal pattern of the September 2024 flood, a recent severe flood event in the study area. The return-period rainfall was estimated by multiplying the ground-gauge rainfall data of the September 2024 flood event by a conversion factor, calculated as the ratio of the return-period rainfall from the frequency curve to the 2-day annual maximum rainfall of the 2024 flood. The flood simulations for each return period were conducted using the rainfall estimated for the corresponding return period.

The impacts of LULC changes on flood runoff, inundation, and volume were analyzed under different LULC scenarios. By overlaying the land-cover maps with delineated flood inundation maps in GIS, the flood-exposed area for each land-cover class was estimated, and the impact of land-cover changes on flood risk was assessed. The calculated flood inundation extent was overlaid on the LULC map to identify areas where different LULC types were exposed to flooding. Subsequently, the area and percentage of each LULC category affected by floods were calculated to quantify flood exposure.

4 RESULTS AND DISCUSSION

4.1 Land-Use and Land-Cover Changes

Figure 3 shows the land-cover maps generated for 2014, 2019, and 2024. Table 1 shows the calculated area of each land-cover class and the changes in area between 2014–2019, 2019–2024, and 2014–2024. The results indicated that the cropland area rapidly decreased, while the built-up area rapidly expanded during the study periods. The built-up area rapidly expanded in the Kathmandu valley, which is located in the upper part of the basin. The cropland area decreased from 1758 km^2 in 2014 to 1731 km^2 in 2019 and to 1560 km^2 in 2024, while the built-up area increased from 104 km^2 in 2014 to 139.7 km^2 in 2019 and to 212 km^2 in 2024. The percentage of the cropland area decreased by 11% from 2014 to 2024, while the percentage of the built-up area increased by 105% from 2014 to 2024. The forest area decreased from 2726 km^2 to 2692 km^2 from 2014 to 2019. However, it increased from 2692 km^2 to 2779 km^2 from 2019 to 2024, because of recent reforestation and conservation efforts in the basin.

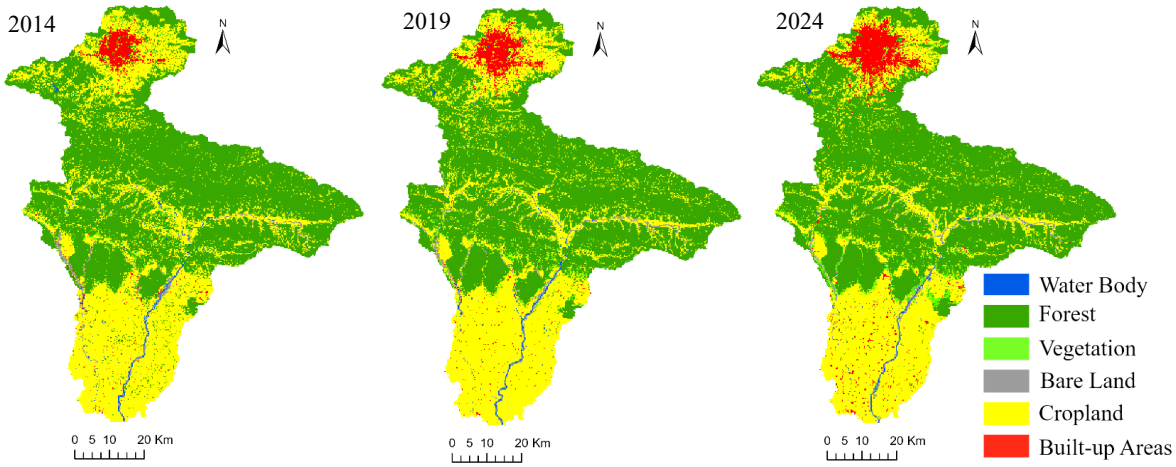

Figure 3: Land-cover maps created for 2014, 2019, and 2024

Figure 4 shows the land-cover maps projected for 2039 and 2049, and Table 2 shows the estimated area of each land-cover class and the estimated changes in area in the future years in comparison with the 2024 data. The cropland area may decrease by 23% in 2039 and by 28% in 2049, compared with the 2024 cropland area, while the built-up area may increase by 66% in 2039 and by 73% in 2049. The lost cropland area was mainly converted to the built-up area. The projected LULC maps for future were based on change trends in LULC for historical periods. The significant changes observed in projected LUCL are based on current change trends that may shift due to socio-economic, climatic, or land use regulation and policy factors.

Table 1 Area of land-cover classes and changes in area between 2014 and 2024

LULC type	Area (km^2)			Change in area (km^2)		
	2014	2019	2024	2014–2019	2019–2024	2014–2024
Water Bodies	34.6	29.5	21	−5.1	−8.5	−13.6
Forest	2726	2692	2779	−34	87	53
Vegetation	36.3	51	85.7	14.7	34.7	49.4
Bare Land	63.8	79.5	65	15.7	−14.5	1.2
Cropland	1758	1731	1560	−27	−171	−198
Built-up Areas	104	139.7	212	35.7	72.3	108

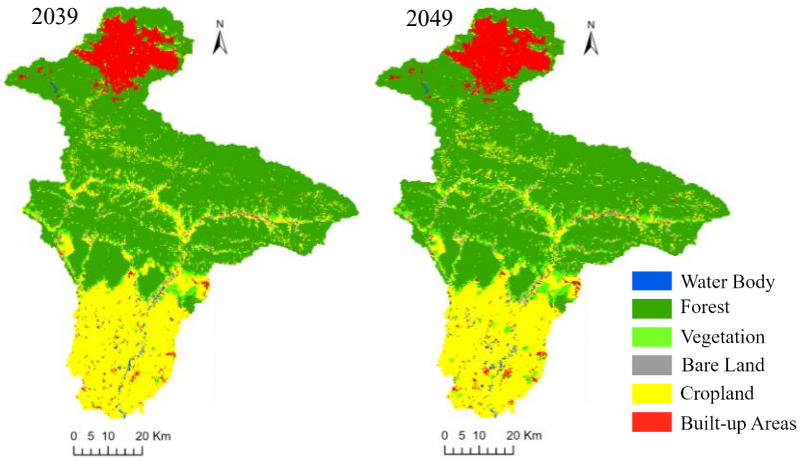

Figure 4: Land-cover maps projected for 2039 and 2049

Table 2 Area of land-cover classes in 2039 and 2049 and comparison with 2024

LULC type	Area (km^2)		Change in area from 2024 (km^2)	
	2039	2049	2024−2039	2024−2049
Water Bodies	19.4	20.9	−1.6	− 0.1
Forest	2896	2898	117	119
Vegetation	180	239	94.3	153
Bare Land	71.3	80.7	6.3	15.5
Cropland	1204	1116	−356	−444
Built-up Areas	352	368	140	156

4.2 Impact of Land-Cover Changes on Flood Risk

Figure 5 compares calculated and observed discharges at the Pandhera Dovan gauging station (calibration with 2004 flood data and validation with 2002, 2014, and 2019 flood data). The results show that the calculated discharges reasonably agree with the observed discharges, indicating high Nash-Sutcliffe Efficiency (NSE) and r-squared values. However, discrepancies between the calculated and observed peak discharges were identified for the 2014 and the second peak in 2019. These discrepancies may be attributed to several possible factors, such as the use of daily rainfall data as model input, limitations in spatial rainfall representation, the quality of topographical data, and potential uncertainties in the discharge-rating curve at high flows. For validation of flood inundation extent, we compared the calculated areas with satellite-based flood observations. Figure 6 shows a comparison between the calculated flood extent area for 2002 flood event and the observed flood inundation extent derived from Moderate Resolution Imaging Spectroradiometer (MODIS) satellite remote sensing (Shrestha, 2019b). The calculated flood inundation extents were very similar to the observed extents by MODIS satellite remote sensing.

Figure 7 compares the calculated discharges using LULC in 2024 and 2049 for the 2024, 50-year, and 100-year floods. The changes in river discharge due to LULC changes are significantly greater at the Khokana station compared with those at the Pandhera Dovan station. Figure 8 shows the time-series inundation volume over the basin, using LULC estimates in 2024 and 2049. The results indicated that the flood inundation volume might also increase in the future due to LULC changes. LULC changes, particularly due to urbanization, lead to increases in river discharge and inundation volume not only during peak flow periods but also during non-peak flow periods. Table 3 summarizes the calculated results of the inundation area and peak inundation volume using LULC estimates in 2024, 2039, and 2049

in the cases of the 2024, 50-year, and 100-year flood events. The rate of increase in flood inundation volume due to LULC changes is comparatively higher than that of flood inundation area, which indicates that most areas of the basin will be flooded to greater depths in the future. In the study area, particularly the Kathmandu valley, located in the upper part of the basin, the built-up area has been significantly expanding, thereby leading to increased river channel encroachment and a higher risk of flooding. The rapid urbanization in the Kathmandu valley may increase river runoff, resulting in greater inundation area and flood inundation volume. The expansion of settlement in flood-prone areas increases the exposure of people and assets to flood damage. Moreover, a significant reduction in cropland has further worsened the flooding situation. LULC changes due to factors such as urbanization, deforestation, and conversion of pervious land to impervious land significantly alter flooding characteristics, increasing the frequency and magnitude of flood events. As a result, the flood risk levels will also change.

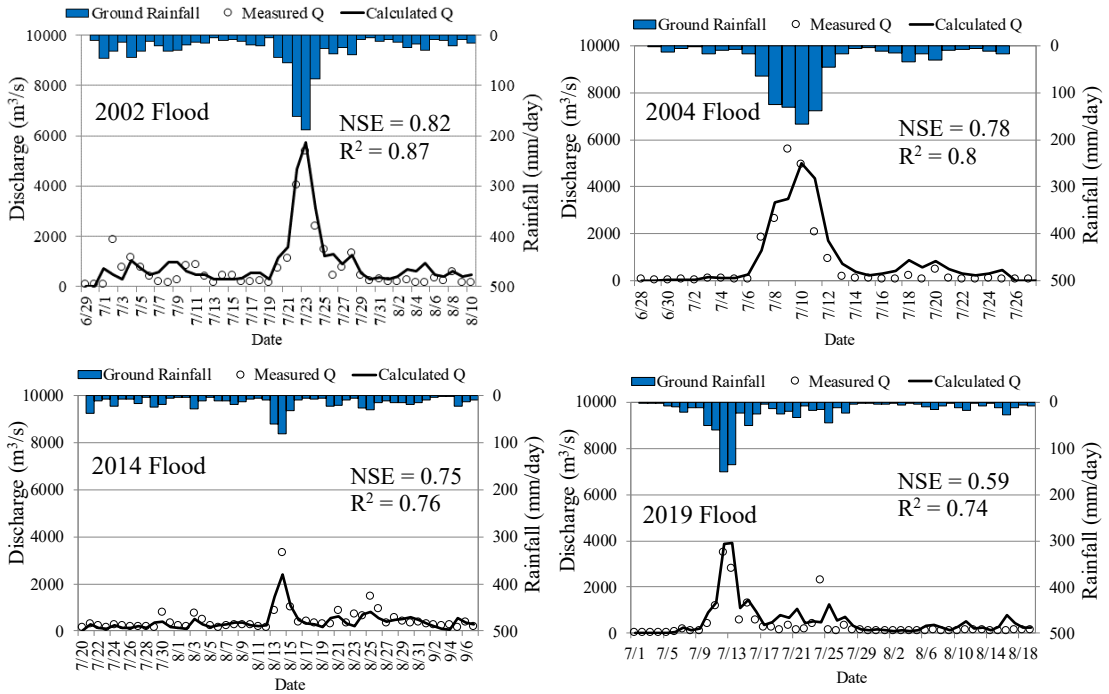

Figure 5: Comparison of calculated and observed discharges at the Pandhera Dovan station (see Fig. 1 for the location of the station

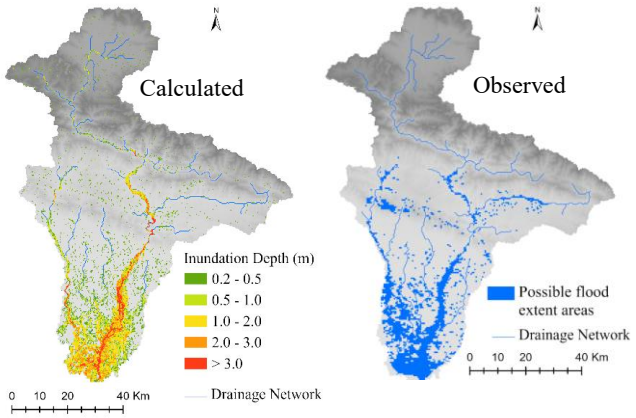

Figure 6: Calculated and satellite-based observed flood extent areas for 2002 flood (Data source for observation: Shrestha, 2019b)

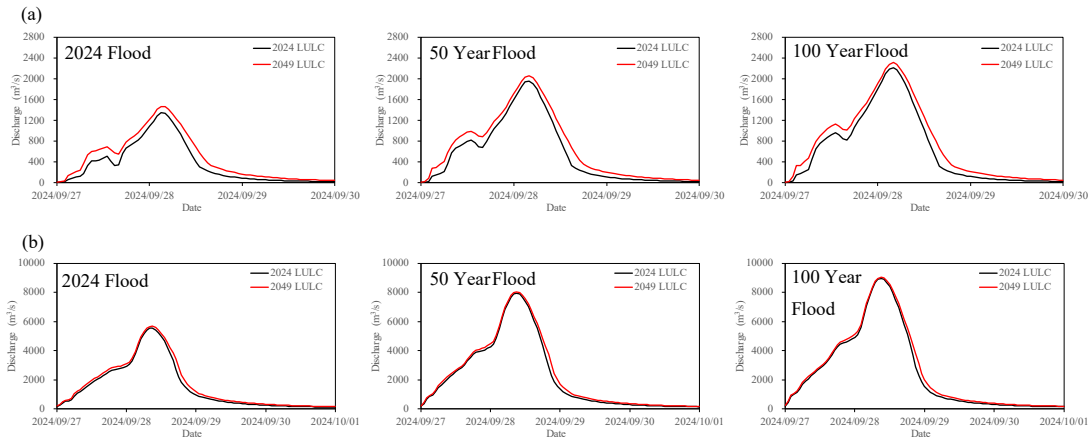

Figure 7: Calculated discharges at the (a) Khokana and (b) Pandhera Dovan stations, using the land-cover maps for 2024 and 2049 (see Figure 1 for the locations)

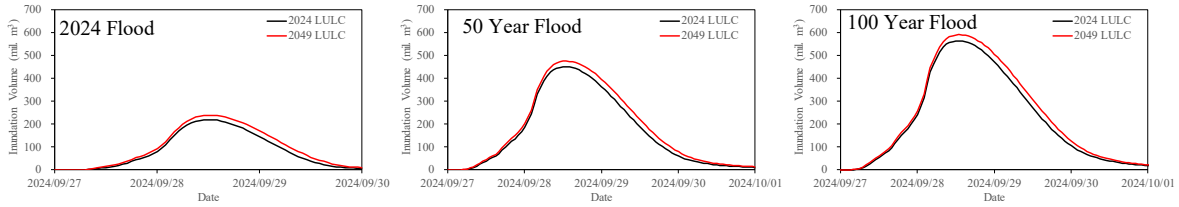

Figure 8: Calculated time-series inundation volumes in the basin, using the land-cover maps for 2024 and 2049

After flood simulations considering the effect of LULC changes, we also estimated inundated area for each land-cover class by overlaying the land-cover maps generated for past and future years with delineated flood inundation maps in GIS. Then, we analyzed the impact of land-cover changes on flood risk. Figure 9 shows the calculated inundated area of each land-cover class for a 100-year flood event under LULC conditions in 2024 and 2049. The results indicated that inundated built-up area may increase by more than 79% under LULC conditions in 2049, because of increases in both flood inundation and exposures in the flood-prone areas, while the flood exposure area of cropland may decrease in the future by 6.3%. This reduction is due to the conversion of cropland to settlement or other land use. The results also indicated that the inundated area of forest and vegetation may also increase in the future.

Table 3 Calculated inundation area and peak inundation volume under current and future land-use and land-cover conditions

LULC year	2024 Flood (11-Year Flood)				50-Year Flood				100-Year Flood			
	Inundation Area		Peak Inundation Volume		Inundation Area		Peak Inundation Volume		Inundation Area		Peak Inundation Volume	
	km^2	% increase with base case	mil. m^3	% increase with base case	km^2	% increase with base case	mil. m^3	% increase with base case	km^2	% increase with base case	mil. m^3	% increase with base case
Using 2024 LULC (base case)	289.5	-	219.1	-	537.4	-	450.2	-	634.9	-	564.8	-
Using 2039 LULC	305.4	5.5	236.3	7.9	551.4	2.6	472.3	4.9	648.8	2.2	588.2	4.2
Using 2049 LULC	307.3	6.2	238.2	8.7	554.5	3.2	474.8	5.5	650.6	2.5	591.2	4.7

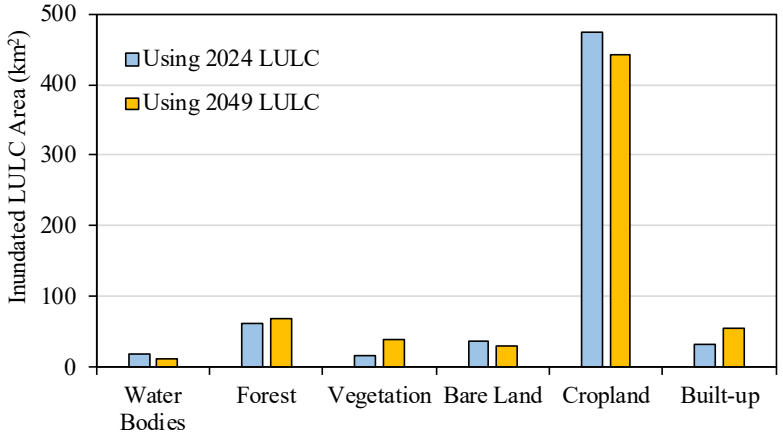

Figure 9: Calculated inundated area of each land-cover class for a 100-year flood under the 2024 and 2049 LULC conditions for flood simulation and exposure assessment

5 CONCLUSIONS

This study analyzed LULC changes in the Bagmati River basin of Nepal using satellite imagery. Land-cover maps for future years were projected using machine learning techniques. Then, the impacts of LULC changes on flooding and flood risk were assessed by coupling hydrologic-hydraulic modelling with exposure assessments under past and future land-cover conditions.

The results indicated that the built-up area, particularly in the Kathmandu valley, located in the upper part of the study basin, is rapidly expanding and may further expand in the future. The percentage of built-up area increased by 105% from 2014 to 2024, and may further increase by 66% in 2039 and by 73% in 2049, compared with the 2024 built-up area. The cropland area is in a declining trend and may continue to decline. The percentage of cropland area decreased by 11% from 2014 to 2024, and may further decrease by 23% in 2039 and by 28% in 2049, compared with the 2024 cropland area. Recently, the forest area in the basin has increased due to reforestation and conservation efforts.

LULC changes in the basin can worsen flooding and increase flood risk. The expansion of the built-up area and the reduction of the cropland area will increase river runoff, flood extent, and flood inundation volume. Changes in river discharge due to LULC changes are significantly greater at the Khokana station, located at the upstream part of the basin, compared with those at the Pandhera Dovan station, located at the middle stream of the basin. The flood inundation extent and the peak inundation volume for a 100-year flood may increase in the future by 2.5% and 4.7%, respectively, due to LULC changes, while they were estimated at 6.2% and 8.7% in the case of the flood scale similar to the recent 2024 event. The inundated built-up area may increase by more than 79% under LULC conditions in 2049, while the flood-exposed cropland area may decrease by 6.3% in the future.

The results indicated that flood runoff, flood extent, and flood inundation volume may increase in the future due to land-cover changes in the basin. The built-up area in the Kathmandu Valley is likely to be exposed to more severe flooding and become more vulnerable to floods due to rapid urbanization, river channel encroachment, and inadequate drainage systems. A large part of cropland is also expected to be exposed to flooding, especially in floodplains in the downstream areas of the basin. This study provides more detailed quantitative link between land-cover changes and hydrological response or risk, and the combined approach of projecting future LULC, analyzing flood impacts, and evaluating class-specific exposure advances current methodologies by linking landscape change directly to flood vulnerability and decision-making. The findings of this study provide useful information for establishing effective land use regulations and flood prevention and adaptation measures.

This study predicted future LULC based on historical LULC change trends. However, future studies should incorporate land-use policies, regulatory or restricted zones, and socio-economic factors to

improve the prediction of future LULC patterns. Furthermore, this study used globally available topographical data for flood simulations across the entire catchment of the study area. The reliability of the simulated flood inundation depth and extent could be improved by incorporating ground-based elevation data.

6 ACKNOWLEDGEMENTS

This work was supported by the Japan Society for the Promotion of Science (JSPS), KAKENHI Research Grant Number 24K07692.

REFERENCES

Banjara M., Bhusal A., Ghimire A.B. and Karla A. (2024). Impact of land use and land cover change on hydrological processes in urban watersheds: analysis and forecasting for flood risk management. Geosciences, 14, 40.

Earth Resources Observation and Science (EROS) Center. (2020). Landsat 8-9 Operational Land Imager / Thermal Infrared Sensor Level-2, Collection 2 [dataset]. U.S. Geological Survey.

Lehner B., Verdin K., Jarvis A. (2008). New global hydrography derived from spaceborne elevation data. Eos, Transactions, American Geophysical Union, 89(10): 93–94.

Martínez-Retureta R., Aguayo M., Stehr A., Sauvage S., Echeverría C. and Sánchez-Pérez J.-M. (2020). Effect of land use/cover change on the hydrological response of a southern center basin of Chile. Water, 12, 302.

Overture Maps Foundation (OMF). (2025). Overture Maps Open Data, https://data.humdata.org/dataset/osgeonepal_npl_roads [accessed on 4 March 2026]

Sayama T., Ozawa G., Kawakami T., Nabesaka S. and Fukami K. (2012). Rainfall-runoff-inundation analysis of the 2010 Pakistan flood 2010 in the Kabul River basin. Hydrol. Sc. J., 57, 298-312.

Shrestha B.B. (2019a). Approach for analysis of land-cover changes and their impact on flooding regime. Quaternary, 2, 27.

Shrestha B.B. (2019b). Assessment of flood hazard and agriculture damage under climate change in the Bagmati River basin of Nepal. Int. J. Environ., 8(2), 55-69.

Wudineh F.A. (2023). Land-use and land-cover change and its impact on flood hazard occurrence in Wabi Shebele River basin of Ethiopia. Hydrology Research, 54(6), 756.

Zhai G., Fukuzono T. and Ikeda S. (2005). Modeling flood damage: case of Tokai Flood 2000. J. Am. Water Resour. Assoc., 41(1), 77-92.